

# **EFFECT OF MATERIAL INSULATION AND PART GEOMETRY ON AC MAGNETIC PERFORMANCE OF P/M SOFT MAGNETIC COMPOSITES**

**L.P. Lefebvre and C. Gélinas\***

**Industrial Materials Institute/National Research Council Canada,  
75 de Mortagne, Boucherville, Québec, Canada J4B 6Y4**

**\* Quebec Metal Powders Limited,  
1655 Marie Victorin, Tracy, Québec, Canada, J3R 4R4**

## **ABSTRACT**

P/M soft magnetic materials intended for AC magnetic applications are generally composed of insulated ferromagnetic particles. The magnetic powder, the insulation and the fabrication process can be varied in order to adjust the material properties to meet the specific requirements of a given application. For example, fine particles and good insulation are generally required to minimize eddy-currents in high frequency applications. At low frequency, insulation is less critical but nevertheless needed in order to minimize the negative effect of the eddy-currents on the magnetization of the material.

In this work, the degree of insulation in magnetic composites and the size of the rings used for the magnetic characterization were varied to study their effect on the magnetic properties. Core losses and electrical resistivity concepts are discussed. The study shows that both resistivity and size may have a significant effect on the apparent permeability (magnetization) and core losses in these materials.

## **1. INTRODUCTION**

Soft magnetic components can be produced to near-net-shape using powder metallurgy (P/M) techniques. Depending on the application, the choice of the material and the processing conditions may differ greatly. For AC applications, ferromagnetic particles must be insulated from each other to create finely subdivided materials that minimize the induction of eddy-currents when exposed to alternating magnetic fields. In most iron-resin composites, it is assessed that the insulation is such that the induction of eddy-currents at low frequency is minimal in standard ring test specimens. However, in real applications, this may be different for larger components, especially when the insulation between the particles is not adequate. When eddy-currents are induced in materials, two main effects are observed: incomplete magnetization of the material (skin effects) and increase in core losses.

This paper describes the effect of insulation and part dimensions on magnetization and core losses. The use of electrical resistivity measurements to evaluate the susceptibility of a material to these parameters is discussed.

## **2. EXPERIMENTAL PROCEDURE.**

For the purpose of this work, three composite materials or dielectromagnetics with different electrical resistivities were pressed at 620 MPa into large discs (20.32 cm by 3.18 cm thick) from which rings of three different sizes were machined. The materials are described in Table 1 together with their density and electrical resistivity after thermal treatment.

**Table 1:** Description of the different materials characterized in this study.

<b>Material</b>	<b>A</b>	<b>B</b>	<b>C</b>
Powder	Iron/resin	Iron/resin	Inorganic-coated iron
Thermal treatment	200°C/1 h	200°C/1 h + 500°C/30 min/air	500°C/15 min + 600°C/30 min/argon
Density, $g/cm^3$	7.22	7.20	6.82
Resistivity, $\mu\Omega\cdot m$	130	4	35

The density and electrical resistivity were evaluated on rectangular specimens machined from the discs (except Material C, where the electrical resistivity was evaluated directly on a ring). Materials A and B had a similar density of about 7.20  $g/cm^3$  while that of Material C was much lower due to the inorganic coating that reduced the compressibility of the powder. The resistivity measured in Material A is typical for these iron/resin composites. For Material B, the purpose of the thermal treatment was to burn off the resin and decrease the resistivity. In the case of Material C, the inorganic coating prevented the formation of electrical contacts between the ferromagnetic particles during the heat treatment even if the temperature was relatively high (up to 600°C). The resistivity of Material C was between those of Material A and B.

Rings of different sizes were machined from these materials, as described in Table 2. Examples of wound rings are shown in Figure 1. The size of the rings was selected in order to get square cross sections and maintain as much as possible a ratio  $D_{in}/D_{ext}$  higher than 0.82 as specified by ASTM A596-89 standard (exception with medium rings made with Material A and B that have a ratio of 0.795).

**Table 2:** Dimensions (cm) of the different rings tested.

<b>Size</b>	<b>Material</b>	<b>Section</b>	<b><math>D_{int}</math></b>	<b><math>D_{ext}</math></b>
Small	A, B, C	0.5 x 0.5	5.24	6.24
Medium	A, B	1.0 x 1.0	7.74	9.74
	C	1.15 x 1.15	14.26	16.58
Large	A, B	1.5 x 1.5	12.24	15.24
	C	1.7 x 1.7	13.19	16.58



**Figure 1:** Three different rings wound for magnetic characterization.

### **3. RESULTS AND DISCUSSION.**

#### ***3.1 Apparent permeability***

The AC apparent permeability of the different rings measured at 0.5 Tesla and at 60 Hz and 400 Hz is given in Figure 2. This apparent permeability is the ratio of the magnetization  $B$  (0.5 T) over the applied field  $H$  (RMS) at a given frequency. This value is not an intrinsic property of the material but gives information on the material characteristics and behavior when exposed to AC magnetic fields. In this study, the lowest permeability is obtained with Material C. This is related to the low density of this material. For the small rings, the highest permeability is obtained with Material B that has a composition similar to Material A. Its higher permeability is attributed to the partial stress relaxation that occurs during the thermal treatment at  $500^{\circ}\text{C}$ . Indeed, it has already been demonstrated that a certain extent of stress relief takes place in these materials treated at temperatures as low as  $450^{\circ}\text{C}$  and this may affect their magnetic properties [1].

The ring cross section or thickness has no significant effect on the AC apparent permeability of Materials A and C at these frequencies. On the other hand, for Material B, which has the lowest resistivity, the apparent permeability decreases with an increase of the cross section, especially at 400 Hz. This is likely due to eddy-currents that impede the complete magnetization of the rings having thick sections. Indeed, it is well known that magnetic fields induced by eddy-currents counteract the magnetizing field causing the field at the surface of the core to be greater than that at the center. This is called the skin effect and makes the AC apparent permeability smaller than the permeability of the material. This effect has been previously observed in magnetic sheets [2], in silicon-iron cores at power frequencies [3] and also in iron-resin composite materials [4].

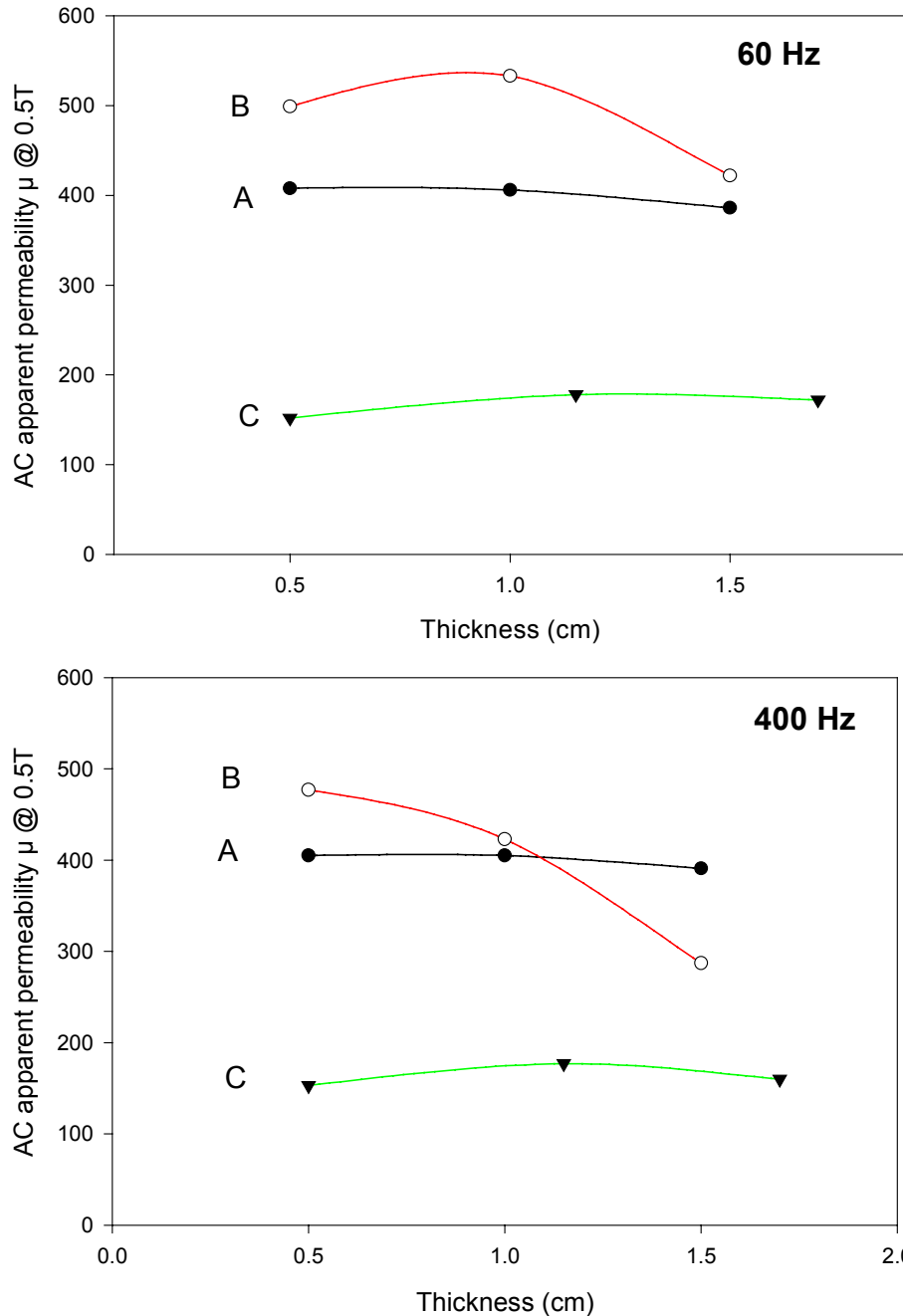


**Figure 2:** AC magnetic permeability at 0.5 Tesla for rings of different thickness fabricated with different materials: 60 Hz (top) and 400 Hz (bottom).

The resistance to the eddy-current flow depends on the electrical resistivity of the conducting phases (magnetic particles in dielectromagnetics) and on the insulation between those phases. In laminations, the insulation between the sheets is usually considered infinite for well-insulated sheets and the electrical resistivity is that of the material of the sheets. In this case, the eddy-current path length is mostly affected by the thickness of the material. However, when the width/thickness ratio of a laminated sheet approaches one, the effect of the width becomes important and has to be considered [5,6].

For large width/thickness ratios, the effect of the eddy-currents on the magnetization may be described using the penetration depth of the magnetic field as a function of the resistivity, permeability and frequency [7]:

$$\delta = K \sqrt{\frac{\rho}{\mu_r f}} \quad (1)$$

where the penetration depth  $\delta$  is defined as the depth in mm where the magnetization equals 1/e the value of the magnetization at the surface of the material,  $\rho$  is the electrical resistivity of the material in  $\mu\Omega\cdot\text{m}$ ,  $\mu_r$  is the permeability,  $f$  is the frequency in Hz and  $K$  is a constant (503 for laminations).

This equation has been developed for homogeneous materials such as steel sheets. It is generally used to determine the sheet thickness required to minimize the skin effects due to the eddy-currents. For dielectromagnetics, the material is inhomogeneous and the physical meaning of  $\delta$  and  $\rho$  is different from that of laminations. In an ideal dielectromagnetic, where monosized spherical magnetic particles would be perfectly insulated from each other,  $\delta$  refers to the penetration in the particle of diameter  $d$  and  $\rho$  to the electrical resistivity of the conducting phase ( $\rho = 0.1 \mu\Omega\cdot\text{m}$  for iron in iron/resin composites).

In reality, dielectromagnetics do not perform accordingly to the ideal model: particle size  $d$  is variable and is difficult to evaluate. Actually, the parameter  $d$  would likely correspond to the diameter of the insulated domains perpendicular to the magnetic field (i.e. eddy-current path length). This value varies from one point to the other in the material and depends on the particle size distribution of the powder and the quality of the insulation between the particles. Thus, the value  $d$  is larger than the particle size of the powder and according to equation 1, skin effects should appear at a much lower frequency than theoretically predicted by equ. 1.

### 3.2 Core losses

Core losses are defined as the power absorbed by a core under stated conditions of applied time varying magnetic field [8]. Different approaches may be used to quantify the core losses when a magnetic material is exposed to alternating magnetic fields. One approach consists of determining the behavior of the material as a function of excitation parameters and material constants. For example, using analytical equations such as the Steinmetz equation, the total power losses  $P_{tot}$  may be expressed as:

$$P_{tot} = n B^{1.6} f + e B^2 f^2 + \text{excess losses} \quad (2)$$

where  $f$  is the frequency,  $B$  the magnetization and  $n$  and  $e$  constants depending on the characteristics of the specimens. The first component is related to the hysteresis portion of the losses, which depends on the structure and composition of the material, the second component is related to the eddy-current losses while the last component refers to the excess losses or anomalous losses. This approach is useful for designers of electromagnetic components and electric devices but gives little information to material scientists on how the material characteristics affect the performance of a component or device.

Equations have been developed to describe the eddy-current losses as a function of material characteristics and microstructure. Using this approach, the magnitude of the losses due to eddy-currents can be calculated or at least approximated under certain restricted conditions (i.e. sinusoidal flux uniformly distributed in the material) as a function of material characteristics. Under these conditions, eddy-current losses in laminations may be determined as [9]:

$$P_{e(sheet)} = \frac{(\pi D f B_m)^2}{6 \rho} \quad (3)$$

where  $D$  is the lamination thickness,  $f$  the frequency,  $B_m$  the peak induction flux and  $\rho$  the electrical resistivity of the material. Similarly, in cylinders or wires of diameter  $D$ :

$$P_{e(cylinder)} = \frac{(\pi D f B_m)^2}{16 \rho} \quad (4)$$

and for spheres of diameter  $D$ :

$$P_{e(sphere)} = \frac{(\pi D f B_m)^2}{20 \rho} \quad (5)$$

More generally, eddy-current losses may be expressed as :

$$P_e = \frac{K (\pi D f B_m)^2}{\rho} \quad (6)$$

where  $D$  is the smallest dimension in the plane of the eddy-current circuits and  $K$  a constant depending on geometrical factors.

There are concerns about the validity of such relationships, especially for dielectromagnetics, due to discrepancies observed between results in laboratory and in real components. Often, discrepancies can be traced back to the non-fulfillment of the basic conditions required for the calculations (sinusoidal flux uniformly distributed throughout the material). They may also come from misinterpretation of the  $\rho$  and  $D$  variables in equation (5). As discussed previously, the electrical resistivity  $\rho$  is that of the conducting phase (0.1  $\mu\Omega$ -m for iron-resin composites) while  $D$ , the diameter of the insulated domains perpendicular to the eddy-current paths, is difficult to determine in dielectromagnetics.

In this study, a material approach was used to interpret the effect of material characteristics on losses in dielectromagnetics. The objective was not to quantify the eddy-current losses but to determine how the material and part characteristics, such as the degree of insulation and geometry, may affect the induction of eddy-currents and the core losses. For instance, in Figure 3, the effect of the cross section of rings fabricated with materials having different electrical resistivities on the apparent core losses at 0.5 T is presented.

Note that the values for the smallest rings (0.5 cm thick) correspond to those usually reported in the literature and obtained on standard test rings. For these rings at 60 Hz, the highest core losses are measured in Material A and the lowest in Material C. It is known that the hysteresis portion of the losses is predominant in these dielectromagnetics at low frequency. Thus, the lowest core losses obtained in Materials B and C result from the thermal treatments at 500°C and 600°C that partially relieved the internal stresses and decreased the hysteresis portion of the losses.

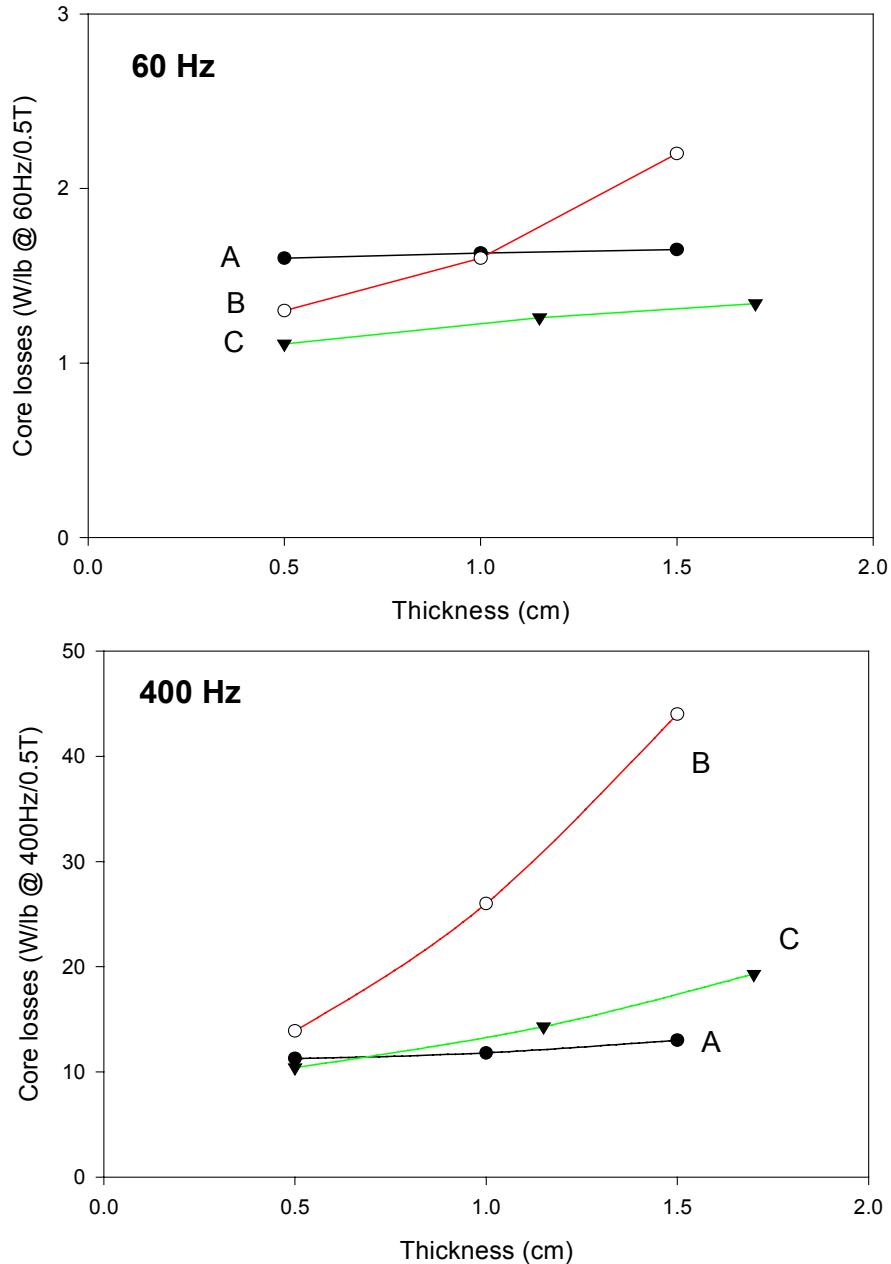


**Figure 3** : Core losses at 0.5 T of rings with different cross sections fabricated with materials with different resistivities: 60 Hz (top) and 400 Hz (bottom).

As the ring cross section and frequency increase, the differences in core losses between the three

materials change a lot. For instance, core losses in Material B increase significantly while those in Material A are almost constant. This is attributed to the lack of insulation between the particles in Material B. In fact, this effect of the geometry should not be related to the hysteresis portion of the losses or the excess losses. Indeed, K.H. Stewart [10] found that excess losses were not dependent on the sheet thickness for laminations and were rather induced by internal friction effects connected with a shift of the Bloch walls during the magnetic cycling. Also, H.J. Williams et al. [11] ascribed these excess losses to inhomogeneous distribution of permeability. Based on these works, it can be assumed that these excess losses are not affected by geometrical factors such as particle size or specimens shape, as long as they do not have an impact on the microstructure of the material and the variation of the losses with the part dimensions comes from the increase of the eddy-currents portion of the losses.

Those losses increase rapidly when material insulation is not sufficient. Consequently, core losses in the largest rings are much higher in Material B. This effect is even worst at 400 Hz, where the eddy-currents are more important. The effect of part dimension and electrical resistivity on the core losses can also be visualized on graphs showing the total losses divided by the frequency as a function of frequency. For instance, in Figure 4, the losses/cycle are plotted versus frequency for rings with different cross sections pressed with Material A and B, having very different electrical resistivities:  $130 \mu\Omega\text{-m}$  and  $4 \mu\Omega\text{-m}$  respectively. The intercept of the plots with the origin (no varying field) is proportional to the hysteresis portion of the losses while the slope depends on the induction of eddy-currents. The hysteresis losses are thus lower in Material B (Fig. 4), which gives a lower value of losses/cycle at the origin. As previously mentioned, this is attributed to the stress relaxation that occurred during the thermal treatment at  $500^\circ\text{C}$ .

In Material A, the slope of the curves corresponding to rings with different cross sections, are rather flat indicating that eddy-currents are very low in these specimens. On the other hand, slopes of the curves for the rings fabricated with Material B are much steeper, especially in larger rings. This indicates that the induction of eddy-currents in this material is more important when the cross section of the specimens increases. For example, core losses at 60 Hz in the large ring are almost twice those in the small ring. This is an indication that the particle insulation in this ring is insufficient to minimize the induction of the eddy-currents.

These results clearly show that the induction of eddy-currents not only depends on the particle size distribution of the powder, the insulation between the particles and the frequency, as suggested by equation (5), but also on specimen geometry. Actually, the lower the electrical resistivity of the material, the more important is the effect of the specimen geometry on the losses.

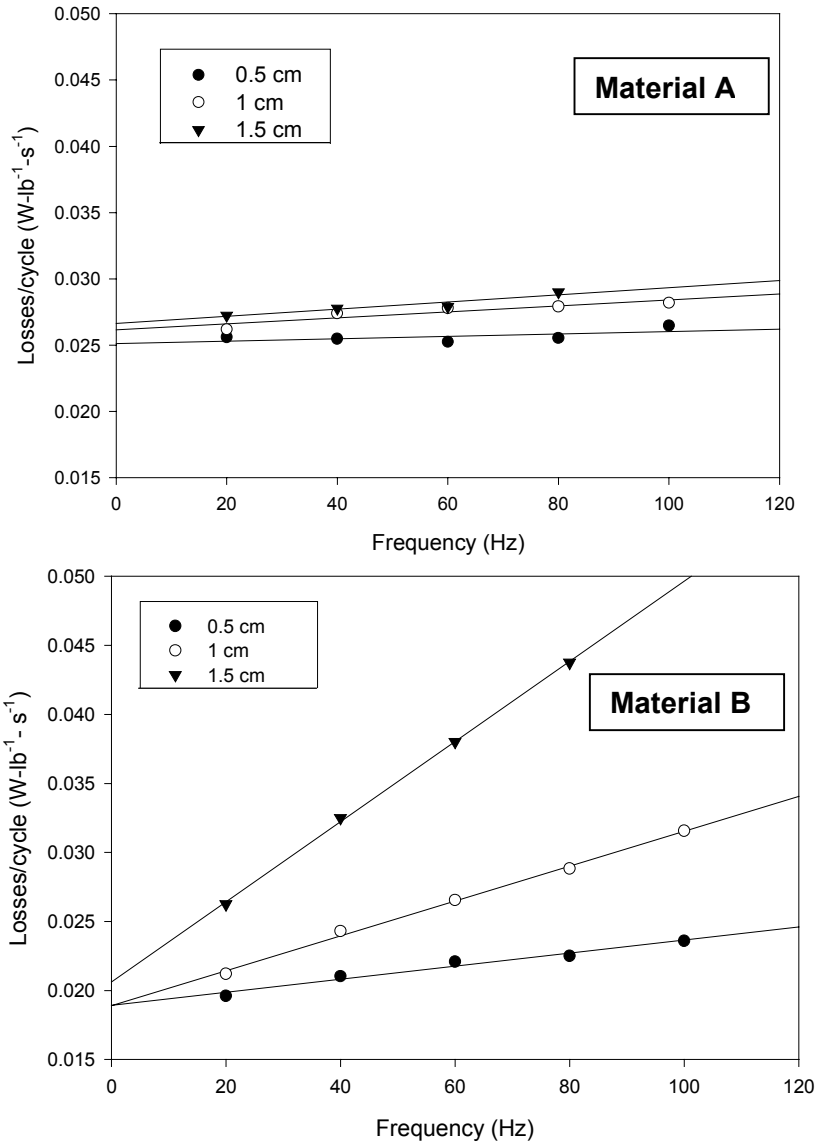


**Figure 4:** Losses per cycle as a function of frequency for rings of different thickness made with Material A (130  $\mu\Omega$ -m top) and Material B (4  $\mu\Omega$ -m bottom).

It appears that the selection of a dielectromagnetic material cannot be based only on the magnetic properties measured on standard ring specimens. For instance, in the present case, Material B would appear as the best material in terms of permeability and core losses measured on small rings (5 x 5 mm). While this material would perform well in small components, it would not be the case in large components, especially if core losses are a major concern for the application. At 60 Hz, Material C would be a good candidate, while at higher frequencies, Material A would be the best material to minimize the core losses in larger components. It is thus believed that a much better appreciation of a material and possible geometric effects is obtained by evaluating the particle insulation together with the magnetic properties. A good way to quantify particle insulation is to evaluate the electrical resistivity of the material.

In the next section, a physical interpretation of the electrical resistivity in dielectromagnetics is

presented. An evaluation of a direct-current measurement method to evaluate the electrical resistivity is also presented and discussed.

### 3.3 Electrical resistivity

The electrical resistivity measured in dielectromagnetics gives an indication of the electrical connectivity between the particles. This value is a bulk evaluation of the resistivity of the material and not the value represented by  $\rho$  in the skin depth and eddy-current equations (equ. 1 and 5), which is the electrical resistivity of the conducting phase ( $\rho = 0.1 \mu\Omega\text{-m}$  for iron-resin composites). A simplified schematic representation of the equivalent electrical circuit in a dielectromagnetic is given in Figure 5a, where black dots and electrical resistances represent the ferromagnetic particles and their interparticle contacts. In Figure 5b, are also illustrated different possible eddy-current paths in a dielectromagnetic.

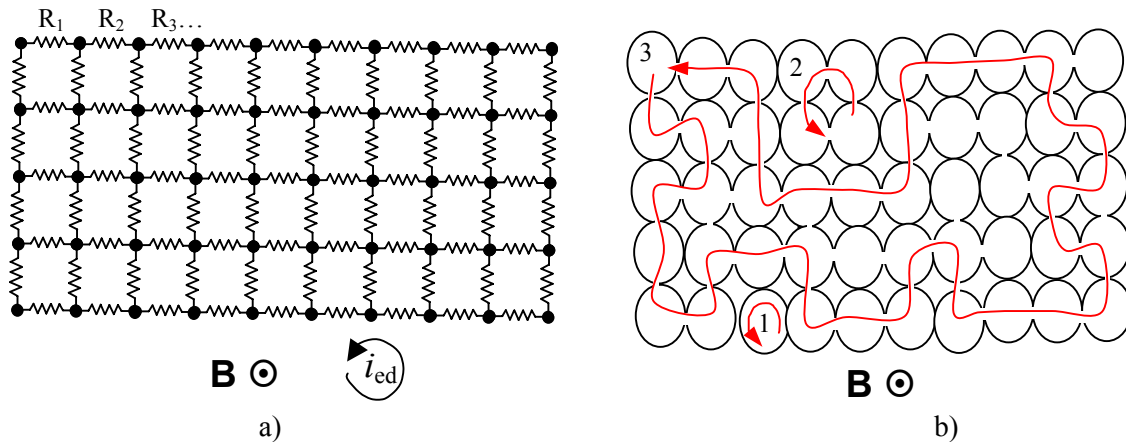


**Figure 5:** Simplified representations of a dielectromagnetic: a) equivalent electrical circuit and b) possible eddy-current paths.

In an ideal dielectromagnetic, the insulation between the particles is perfect and the electrical resistance of the contacts is infinite compared to the electrical resistivity of the conduction phase. In this case, the value  $D$  in equation (5) corresponds to the size of the particles and the eddy-current path is restricted within the particle (circuit #1 in Fig. 5b). When metallic contacts are created between adjacent particles (e.g., during compaction and thermal treatment), resistance decreases and electric currents may flow from one particle to the others. In this case, the value  $D$  corresponds to the size of the agglomerate of contacting particles and the eddy-current path enlarges (circuit #2 in Fig. 5b). When the insulation is not perfect, currents may find their way throughout the whole specimen, as illustrated by the circuit #3 in Fig. 5b. If there is no insulation between particles, such as in sintered components,  $D$  corresponds to the part thickness. In dielectromagnetics,  $D$  values between these two extreme cases can exist in the same material.

Actually, the size of the eddy-current domains may be expressed as a continuum of  $D$  values ranging from the particle size of the powder to the cross section of the component. It is practically very difficult to evaluate the size of these domains  $D$ . However, the electrical resistivity of the material may be used to obtain an indication of the degree of interparticle insulation. For instance, in case of poor insulation (many particle-to-particle contacts), the electrical resistivity is low and the amount of induced eddy-currents circulating in the whole material is more important. The

effect of these currents increases with part dimensions.

Direct-current measurement methods, which measure voltage drop between electrodes, are traditional methods used to evaluate materials resistivity [12]. The four-point contact probe method is one of the techniques extensively used to measure the electrical resistivity of materials. The principle of the method is illustrated in Figure 6. A more detailed description of the experimental technique for electrical resistivity measurements using four-point contact probes is given elsewhere [13,14].

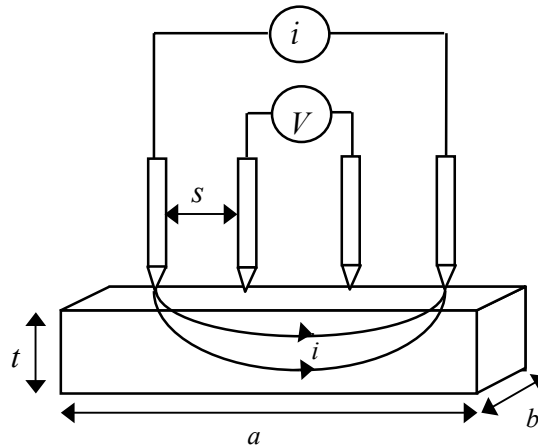


**Figure 6:** Schematic of the four-point contact direct-current measurement method.

Electric resistivities are calculated using the values of current and voltage drop measured between the probes. The equation used for the calculation of the electrical resistivity depends on the specimen geometry and probe spacing  $s$ . For different measurement configurations on rectangular bars, the equations are:

$$\text{For } t < s/2 \quad \rho = R t \frac{\pi}{\ln(2)} C_s \quad (7)$$

where  $\rho$  is the resistivity ( $\mu\Omega\text{-m}$ ),  $R$  is the resistance ( $\mu\Omega$ ) measured with a micro-ohmmeter,  $t$  is the thickness of the specimen and  $C_s$  is a constant depending on  $a$ ,  $b$  and  $s$  (see Fig.6).

$$\text{For } t > 3s \quad \rho = 2 \pi s R C_s \quad (8)$$

$$\text{and for } s/2 < t < 3s \quad \rho = \frac{R \pi t}{\ln(2)} C_t C_s \quad (9)$$

where  $C_t$  is a constant depending on  $s$  and  $t$  (see Fig.6). For example, for standard TRS bars ( $t = 6.4$  mm,  $a = 31.8$  mm,  $b = 12.7$  mm) and a probe spacing  $s$  of 8 mm, equation (9) can be applied with  $C_t = 0.9666$  and  $C_s = 0.3483$ .

In order to assess the validity of the measurements using different probes and calculation equations, the electrical resistivity was measured on standard TRS bars machined from wrought Inconel 600 using probes with a different spacing  $s$ : 1.27 mm, 2.54 mm and 8 mm. The results are presented in Figure 7. The electrical resistance was measured using a micro-ohmmeter (UltraOptec PMO 450) and the three different probes. The measured resistivity value is close to

that found in literature, about  $1.03 \mu\Omega\text{-m}$  [15], and there is no significant difference between the values obtained with the three probes, indicating that the method is accurate and reproducible using the different probes and their corresponding calculation equations.

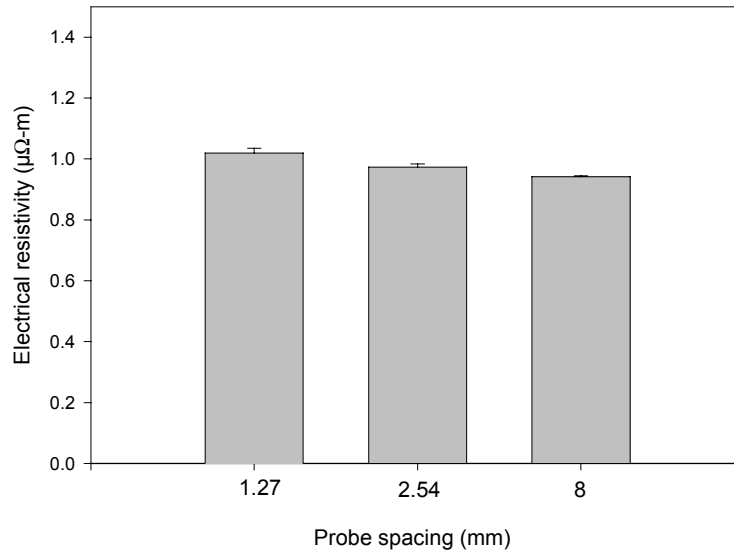


**Figure 7:** Effect of probe spacing on the electrical resistivity measurement carried out on wrought Inconel 600.

Contrary to the Inconel wrought material, dielectromagnetics are inhomogeneous materials composed of a conducting phase, the magnetic particles, and an insulating phase, the dielectric. The four-point direct-current method can nevertheless be applicable for dielectromagnetics if two criteria are respected: the induced currents must travel a distance significantly larger than the heterogeneity (discrete particles) and throughout the bulk material (not only on the surface).

In order to validate this concept, the electrical resistivity of an iron-resin composite was evaluated using the three different probes. Measurements were carried out on iron-resin composite bars (5 specimens) after a curing treatment at  $175^\circ\text{C}$  for 30 minutes in air. The effect of the surface preparation was also evaluated by polishing the top and bottom faces using a 240 grit sand paper in two different directions: parallel to the  $a$  and  $b$  axis (see Figure 6). For each specimen, 5 readings were taken on the top and bottom faces and averaged. The results obtained with the different probes are given in Figure 8.

The resistivity values obtained using the 1.27 mm probe spacing are highly affected by the surface condition of the specimens. The highest values are obtained on the as-cured bars (about  $935 \mu\Omega\text{-m}$ ) and the lowest on the bars polished parallel to the  $b$  axis (about  $260 \mu\Omega\text{-m}$ ). Differences and variations are very large and make the interpretation of the electrical resistivity of the material very difficult.

On the other hand, both the variations and the effect of the surface preparation decrease with an increase of the probe spacing. For the 8 mm probe spacing, values around  $230 \mu\Omega\text{-m}$  are obtained whatever the surface preparation. This suggests that the depth of penetration of the electrical currents is critical for the measurements in these composite materials. For instance, with a small probe spacing, the volume analyzed is small and the resistance is strongly affected by surface heterogeneities (resin concentration, number of particles or interfaces, oxidation, ...). When the probe spacing increases, the resistance becomes less dependent on surface heterogeneities because

the penetration depth of the electric current increases and the volume analyzed enlarges, as illustrated in Figure 9. Consequently, measured values become more representative of the bulk properties of the material.

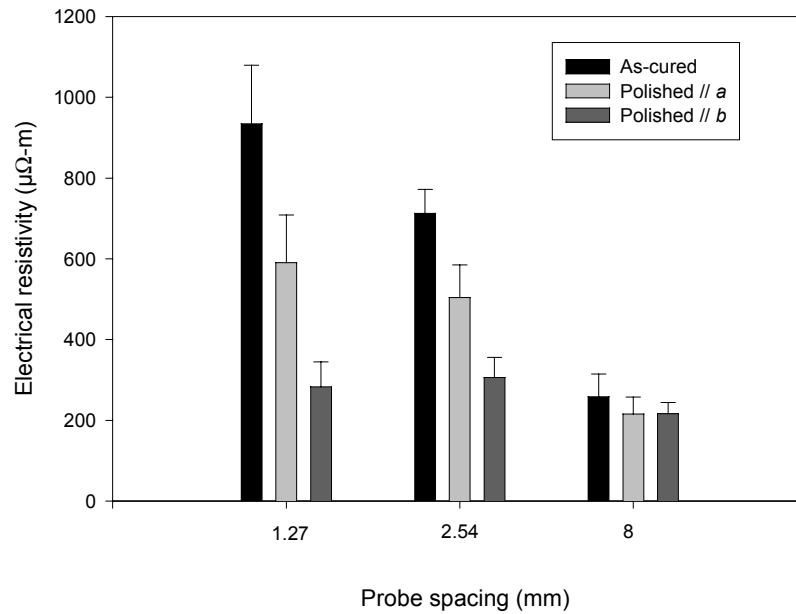


**Figure 8:** Effect of probe spacing and specimen preparation on the electrical resistivity measurements carried out on iron-resin bars.



**Figure 9:** Effect of probe spacing on the penetration of the electric current and the volume analyzed.

Tests were also done to evaluate if the currents did in fact penetrate the entire specimens for the large probe spacing used. Results showed that the electric resistance measured was significantly higher after machining 1 mm from the bottom face of the specimens. This indicates that the whole cross section contributes to the flow of the current and the currents did in fact penetrate the entire specimen for the test conditions used.

Thus, this method commonly used to evaluate the resistivity of different types of materials may also be used for dielectromagnetics. Surface effects can be minimized by selecting the appropriate probe and specimen geometry, ensuring that current penetrates throughout the material.

#### **4. CONCLUSION**

It has been discussed how insulation in dielectromagnetics and part geometry relate to skin effects (incomplete magnetization) and core losses, using a materials approach. It appears that the magnetic properties generated from standard test specimens do not provide sufficient information on the material performance. Dielectromagnetics are used in a variety of applications where shape or size, frequency, magnitude and orientation of the magnetic excitation greatly differ. Quantification of the degree of insulation in these materials is thus necessary in order to fully evaluate the magnetic performances of real components. It has been shown that the four-point direct-current method is adequate to evaluate the electrical resistivity of dielectromagnetics using the appropriate probe spacing and specimen geometry.

Electrical resistivity gives a good indication of the connectivity of the magnetic particles and the material susceptibility to the induction of eddy-currents. For instance, in a low resistivity material (poor insulation), eddy-currents can circulate in the whole specimen and the part size or geometry has an impact on the magnetic properties. This effect is more important when the frequency increases and the electrical resistivity decreases.

Data collected from the resistivity and magnetic characterization could be very useful as long as their physical meaning is clearly understood. For example, relative material performances under specific conditions could be extrapolated from these data. The minimum electrical resistivity required to minimize the induction of eddy-currents could thus be determined for a given part dimension, field induction and frequency using these data.

#### **ACKNOWLEDGEMENTS**

The authors greatly acknowledge Mr. G. St-Amand for his contribution to the experimental work and Mr. R. Dubuc from IREQ for his help in the magnetic characterization.

#### **REFERENCES**

- <sup>1</sup> L.P. Lefebvre, I.P. Swainson, Y. Deslandes, G. Pleizier and P. Chartrand, "Microstructure and Properties of Heat Treated Iron Powder Compacts Intended for AC Magnetic Applications", *Materials Science and Technology*, Vol. 17, No.1, 2001, pp.45-53.
- <sup>2</sup> C. Heck, *Magnetic Materials and their Applications*, Crane, Russak & Co, Inc, New-York, 1974, 50.
- <sup>3</sup> D. Zhang, "Magnetic Skin Effect in Silicon-Iron Core at Power Frequency", *J. of Magn. & Magn. Mat.*, 221, 2000, pp.414-416.
- <sup>4</sup> L.-P. Lefebvre, S. Pelletier, B. Champagne and C. G elinas, , "Effect of Resin Content and Iron Powder Particle Size on Properties of Dielectromagnetics", in *Advances in Powder Metallurgy & Particulate Materials*, 1996, MPIF, Princeton,N.-J., p.20-47.
- <sup>5</sup> R. Aouli, M. Akroune-M; M.A. Dami-MA and A. Mouillet-A, "Iron loss measurement device under rotating magnetic field", in *IEE Proceedings Science, Measurement and Technology*. Vol.146, No.1; 1999; p.35-9.

- 
- <sup>6</sup> T. Chevalier, A. Kedous-Lebouc and B. Cornut, “Influence of Electrical Sheet Width on Dynamic Magnetic Properties”, *J. Magn. & Magn. Mat.*, 215, 2000, pp.623-625.
- <sup>7</sup> C. Heck, *Magnetic Materials and their Applications*, Crane, Russak & Co, Inc, New-York, 1974, p.674.
- <sup>8</sup> IEEE Standard for Test Procedures for Magnetic Cores, IEEE Std 393-1991.
- <sup>9</sup> R.M. Bozorth, *Ferromagnetism*, IEEE Press, NJ, 1993, p.778.
- <sup>10</sup> K.H. Stewart, Losses in Electrical Sheet Steel, in *Proc. IEE*, Vol.2, No. 97, 1950, pp.121-125.
- <sup>11</sup> H.J. Williams, W. Shockley and C. Kittel, “Studies of the Propagation Velocity of a Ferromagnetic Domain Boundary”, *Phys. Rev.* 80, 1959, pp.1090-1094.
- <sup>12</sup> ASTM A 712-97: Standard Test Method for Electrical Resistivity of Soft Magnetic Alloys.
- <sup>13</sup> F. M. Smits, “Measurements of Sheet Resistivities with the Four-Point Probe”, *Bell System Technical Journal*, 37, 1958, , p.711.
- <sup>14</sup> A. Uhlir, Jr., “The Potential of Infinite Systems of Source and Numerical Solutions of Problems in Semiconductor Engineering”, *Bell System Technical Journal*, 34, 1955, p.105.
- <sup>15</sup> *Smithells Metals Reference Book*, Sixth Edition, Edited by Eric A. Brandes, Published by Butterworth & Co, 1983, pp.14-20.